

****FULL TITLE****
*ASP Conference Series, Vol. **VOLUME**, **YEAR OF PUBLICATION***
****NAMES OF EDITORS****

On the Origin of Strong-Field Polarity Inversion Lines

B. T. Welsch¹ and Y. Li¹

Abstract. Several studies have correlated observations of impulsive solar activity — flares and coronal mass ejections (CMEs) — with the amount of magnetic flux near strong-field polarity inversion lines (PILs) in active regions’ photospheric magnetic fields, as measured in line-of-sight (LOS) magnetograms. Practically, this empirical correlation holds promise as a space weather forecasting tool. Scientifically, however, the mechanisms that generate strong gradients in photospheric magnetic fields remain unknown. Hypotheses include: the (1) emergence of highly twisted or kinked flux ropes, which possess strong, opposite-polarity fields in close proximity; (2) emergence of new flux in close proximity to old flux; and (3) flux cancellation driven by photospheric flows acting fields that have already emerged. If such concentrations of flux near strong gradients are formed by emergence, then increases in unsigned flux near strong gradients should be correlated with increases in total unsigned magnetic flux — a signature of emergence. Here, we analyze time series of MDI line-of-sight (LOS) magnetograms from several dozen active regions, and conclude that increases in unsigned flux near strong gradients tend to occur during emergence, though strong gradients can arise without flux emergence. We acknowledge support from NSF-ATM 04-51438.

1. Strong gradients across PILs

It has been known for decades that flares and filament eruptions (which form CMEs) originate along polarity inversion lines (PILs) of the radial photospheric magnetic field. In studies using photospheric vector magnetograms, Falconer *et al.* (2003, 2006) reported a strong correlation between active region CME productivity and the total length of PILs with strong potential transverse fields (> 150 G) and strong gradients in the LOS field (greater than 50 G Mm^{-1}). They used a ± 2 -day temporal window for correlating magnetogram properties with CMEs. Falconer *et al.* (2003) noted that these correlations remained essentially unchanged for “strong gradient” thresholds from 25 to 100 G Mm^{-1} . Using more than 2500 MDI (LOS) magnetograms, Schrijver (2007) found a strong correlation between major (X- and M-class) flares and the total unsigned magnetic flux near (within ~ 15 Mm) strong-field PILs — defined, in his work, as regions where oppositely signed LOS fields that exceed 150 G lie closer to each other than the instrument’s ~ 2.9 Mm resolution. Schrijver’s (2007) effective gradient threshold, $\sim 100 \text{ G Mm}^{-1}$, is stronger than that used by Falconer *et al.* (2003, 2006).

Although these studies were published recently, the association between flares and δ sunspots, which possess opposite-sign umbrae within the same penum-

¹Space Sciences Laboratory, University of California, 7 Gauss Way, Berkeley, CA 94720-7450

bra — and therefore also possess strong-field PILs — has been well known for some time (Künzel 1960; Sammis *et al.* 2000). In particular, $\beta\gamma\delta$ spot groups are most likely to flare (Sammis *et al.* 2000). A $\beta\gamma$ designation means no obvious north-south PIL is present in an active region (Zirin 1988).

We note that Cui *et al.* (2006) found that the occurrence of flares is correlated with the maximum magnitude of the horizontal gradient in active region LOS magnetograms — not just near PILs — and that the correlation increases strongly for gradients stronger than $\sim 400 \text{ G Mm}^{-1}$.

One would expect the measures of CME- and flare- productivity developed by both Falconer *et al.* (2003,2006) Schrijver (2007) to be larger for larger active regions. Importantly, however, both studies showed that their measures of flux near strong-field PILs is a better predictor of flare productivity than total unsigned magnetic flux. Evidently, more flux is not, by itself, as significant a predictor of flares as more flux near strong-field PILs.

These intriguing results naturally raise the question, “How do strong-field PILs form?” For brevity, we hereafter refer to strong-field PILs as SPILs.

Schrijver (2007) contends that large SPILs form primarily, if not solely, by emergence. But he also noted that flux emergence, by itself, does not necessarily lead to the formation of SPILs. Rather, a particular type of magnetic structure must emerge, one containing a long SPIL at its emergence. He suggests such structures are horizontally oriented, filamentary currents.

Beyond the “intact emergence” scenario presented by Schrijver (2007), other mechanisms can generate SPILs. When new flux emerges in close proximity to old flux — a common occurrence (Harvey and Zwaan 1993) — SPILs can form along the boundaries between old and new flux systems. Converging motions in flux that has already emerged can also generate SPILs. If the convergence leads to flux cancellation by some mechanism — emergence of U loops, submergence of inverse-U loops, or reconnective cancellation (Welsch 2006) — then the total unsigned flux in the neighborhood of the SPIL might decrease as the SPIL forms. We note that, while cancellation in already-emerged fields can occur via flux emergence (from upward moving U-loops), the emergence of a new flux system across the photosphere must increase the total unsigned flux that threads the photosphere.

If the emergence of new flux were primarily responsible for SPILs, then a straightforward prediction would be that an increase in total unsigned flux should be correlated with an increase in the amount of unsigned flux near SPILs. Hence, observations showing that increases in the unsigned flux near SPILs frequently occur without a corresponding increase in total unsigned flux would rule out new flux emergence as the sole cause of these strong field gradients.

Our goal is to investigate the relationship between increases in the amount of unsigned flux near SPILs with changes in unsigned flux in the active regions containing the SPILs, to determine, if possible, which processes generate SPILs.

2. Data

From days-long time series of deprojected, 96-minute, full-disk MDI magnetograms for $N_{AR} = 64$ active regions, we computed the rates of change of unsigned flux near SPILs, following the method described by Schrijver (2007). We

also computed the rates of change of total unsigned line-of-sight magnetic flux these active regions.

Our active region sample was chosen for use in a separate study of the relationships between surface flows derived from magnetograms and CMEs. For the purposes of that study, we typically selected active regions with a single, well defined PIL, for ease in identifying the presence of shearing and/or converging flows some CME models employ (Antiochos *et al.* 1999; Linker *et al.* 2001). The sample used here includes regions from 1996 - 1998, and includes regions that did and did not produce CMEs. Some of our magnetograms image the same active region as it rotated back onto the disk one or more times. Also, some of our selected regions are so decayed that they lack spots, and therefore have no NOAA designation.

Here, we analyze $N_{\text{mag}} = 4062$ magnetograms. Pixels more than 45° from disk center were ignored. To convert the LOS field, B_{LOS} , to an estimated radial field, B_R , cosine corrections were used, $B_R = B_{\text{LOS}}/\cos(\Theta)$, where Θ is the angle from disk center.

Triangulation was used to interpolate the B_R data — regularly gridded in the plane-of-sky, but irregularly gridded in spherical coordinates (θ, ϕ) on the solar surface — onto points (θ', ϕ') corresponding to a regularly gridded, Mercator projection of the spherical surface. This projection was adopted because it is conformal (locally shape-preserving), necessary to ensure displacements measured in the tracking study mentioned above were not biased in direction. For computing gradients, a conformal projection is also appropriate. The background grayscale in Figure 1 is a typical reprojected magnetogram. We note that the price of preserving shapes in the deprojection is distortion of scales; but this can be easily corrected.

Each active region was tracked over 3 - 5 days, and cropped with a moving window. A list of tracked active regions and mpeg movies of the active regions, are online, at <http://sprg.ssl.berkeley.edu/~yanli/lct/>.

3. Analysis methods

To identify SPILs, we used the gradient identification technique of Schrijver (2007). For a magnetogram at time t_i , binary positive/negative strong-field masks — where $B_R > 150$ G and $B_R < -150$ G, respectively — were constructed, then dilated by a (3x3) kernel to create dilated positive and negative bitmaps, M_{\pm} . These procedures are illustrated in Figure 1. Regions of overlap, where $M_{\text{OL}} = M_+M_- = 1$, were identified as SPILs. In Figure 1, $M_{\text{OL}} \neq 0$ for a single pixel, at $(x, y) = (112, 91)$.

To quantitatively define neighborhoods around SPILs, M_{OL} is convolved with a normalized Gaussian,

$$G(u, v) = G_0^{-1} \exp(-[u^2 + v^2]/2\sigma^2) \quad (1)$$

where $G_0 = \int du \int dv \exp(-[u^2 + v^2]/2\sigma^2)$, and $\sigma = 9$ pixels (corresponding to a FWHM $\simeq 15$ Mm at disk center), to create “weighting maps,” C_{MG} , where

$$C_{MG}(x, y) = \text{convol}(M_{\text{OL}}(x, y), G) . \quad (2)$$

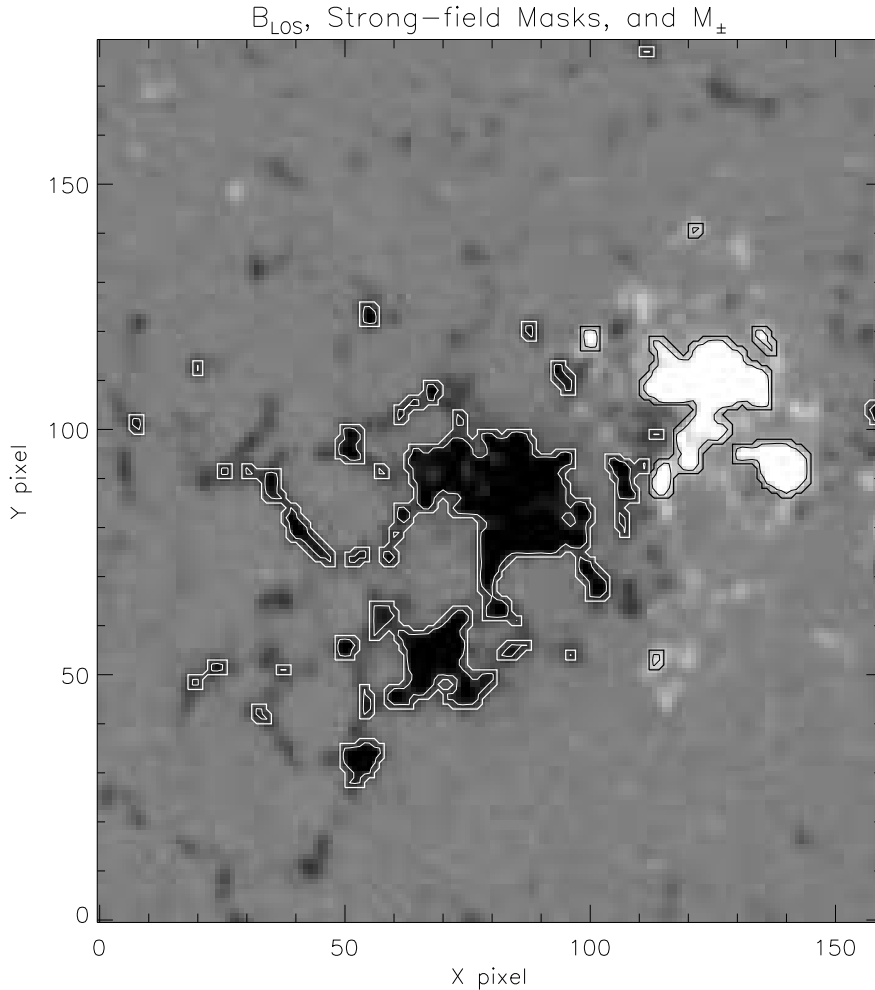


Figure 1. The background grayscale is typical, reprojected magnetogram; white is positive flux, black is negative flux. The inner black and white contours enclose signed, strong-field masks — regions where $B_R > 150$ G and $B_R < -150$ G (respectively). The outer black and white contours show the outlines of M_{\pm} , dilated bitmaps of the strong-field masks with a 3×3 kernel function. For this magnetogram, the dilated bitmaps overlap at a single pixel, at $(x, y) = (112, 91)$.

Figure 2 shows the product of B_R with such a weighting map. Following Schrijver (2007), we totaled the unsigned magnetic field over the weighting map to determine R , a measure of the unsigned flux near SPILs,

$$R = \sum |B_R| C_{MG} . \quad (3)$$

From a sample of more than 2500 MDI magnetograms, Schrijver (2007) showed that R is correlated with major (X- and M-class) flares.

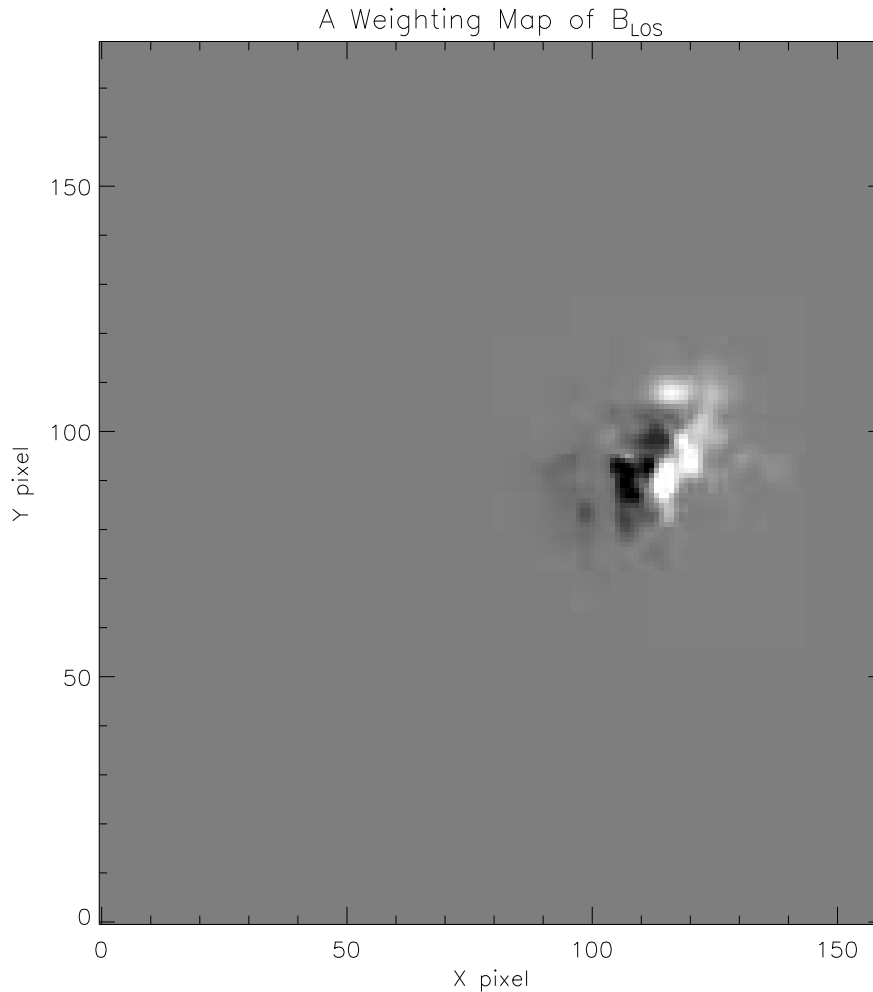


Figure 2. B_R multiplied by a weighting map, C_{MG} . R is the total unsigned field the window, $\sum |B_R| C_{MG}$.

For each of the $N_R = 1621$ magnetograms with $R \neq 0$, we summed the weighted absolute magnetic field in the previous magnetogram, $B_R(t_{i-1})$, using the weighting map from t_i , to compute the backwards-difference ΔR ,

$$\Delta R = \sum (|B_R(t_i)| - |B_R(t_{i-1})|) C_{MG} . \quad (4)$$

We also computed the change in summed, unsigned field,

$$\Delta \mathcal{B} = \sum (|B_R(t_i)| - |B_R(t_{i-1})|) , \quad (5)$$

to determine if new flux is emerging or if flux is canceling. If new flux is emerging, we expect $\Delta \mathcal{B} > 0$. If flux is canceling, we expect $\Delta \mathcal{B} < 0$. Like Schrijver (2007), we have opted to keep R in units of flux density; for simplicity, we also keep $\Delta \mathcal{B}$ in these same units.

When the overlap map M_{OL} for $B_R(t_i)$ is identically zero, R is also zero, and ΔR and $\Delta \mathcal{B}$ are not computed.

In §1. we discussed processes that can cause changes in R . What processes can lead to $\Delta \mathcal{B} \neq 0$? Emergence of new flux or cancellation (both only happen at PILs) can make $\Delta \mathcal{B} \neq 0$, and these processes are probably related to evolution in R . Flux can also cross into or out of the cropping window. Since our cropping windows were selected to include essentially all of each tracked active region’s flux, systematic errors arising in this way are expected to be small. A more severe effect is the “unipolar appearance” phenomenon characterized by Lamb *et al.* (2007), who found that the majority of newly detected flux in the quiet sun is due to coalescence of previously existing, but unresolved, single-polarity flux into concentrations large and strong enough to detect. While it is unclear if the conclusion reached by Lamb *et al.* (2007) for the quiet sun also applies in active regions, this is plausible. Moreover, much as flux can “appear,” flux can also disappear, via dispersive photospheric flows or perhaps even molecular diffusivity. Also, simultaneous emergence of new flux and cancellation of existing flux can occur within the same active region, masking the effects of both processes. Practically, therefore, we can only refer to increases in unsigned flux as “possible new flux emergence,” and to decreases in unsigned flux as “possible cancellation.”

4. Results and conclusions

In Figure 3, we show a scatter plot of changes in R as a function of changes in \mathcal{B} . The plot does not show the full range in $\Delta \mathcal{B}$, but the ΔR for outliers on the horizontal axes are near zero. One striking feature of the plot is its flatness, i.e., that most changes in \mathcal{B} are not associated with any change in R . In Table 1, we tabulated the data points in each quadrant of this plot. Clearly, increases in R , the unsigned flux near SPILs, usually occur simultaneously with increases in the unsigned flux over the entire active region. Increases in R only occur less frequently when flux is decreasing, i.e., during cancellation.

Table 1. Breakdown of Flux Changes

	$\Delta \mathcal{B} < 0$	$\Delta \mathcal{B} > 0$
$\Delta R > 0$	215	671
$\Delta R < 0$	363	371

We set out to answer the question, “How do strong-field PILs form?” We related changes in total, unsigned flux over whole active regions with changes in total, unsigned flux in subwindows of the same active regions — defined by weighting maps. One might expect, therefore, that these quantities should be correlated, casting doubt about our ability to discriminate between changes in total flux in active regions and in subwindows. If the two were strongly correlated, the excess of events with $\Delta R > 0$ and $\Delta \mathcal{B} > 0$ might not be very meaningful. In fact, however, ΔR and $\Delta \mathcal{B}$ are poorly correlated: the two have a linear correlation coefficient $r = 0.29$, and a rank-order coefficient of 0.36. This suggests that the relationship between increases in R and increases in total, unsigned active region flux is not an artifact of our approach.

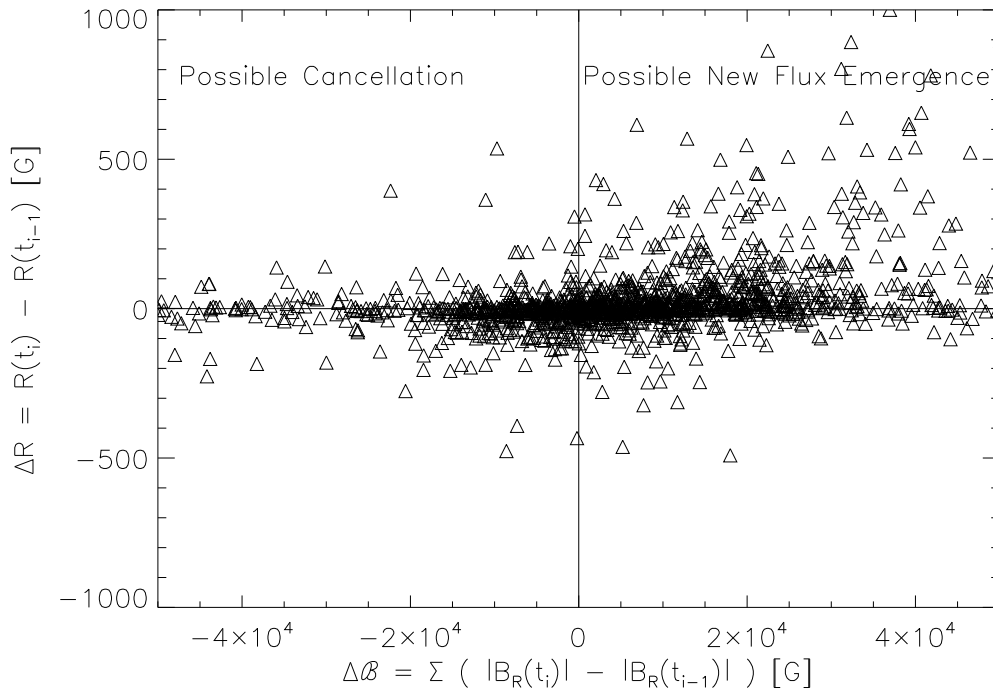


Figure 3. A scatter plot of changes in R as a function of changes in B . Increases in R , the unsigned flux near SPILs, usually occur simultaneously with increases in the unsigned flux over the entire active region. Increases in R only occur rarely when flux is decreasing, i.e., during cancellation. For a breakdown of the data points in each quadrant, see Table 1.

Nonetheless, our active region sample is not ideally suited to address the origin of SPILs, generally. Our sample was not unbiased with respect to active region morphology; we selected regions with well-defined PILs. In addition, our sample included some decayed active regions that NOAA AR designations. Consequently, we believe that a follow-up study, with a much larger, unbiased sample of active regions, is warranted.

With caveats, therefore, our study supports Schrijver's (2007) contention that the emergence of new flux creates the strong-field polarity inversion lines that he found to be correlated with flares.

Acknowledgments. We acknowledge the support of NSF Grant NSF-ATM 04-51438.

References

- Antiochos, S. K., DeVore, C. R., and Klimchuk, J. A. 1999, *ApJ* 510, 485.
 Cui, Y., Li, R., Zhang, L., He, Y., and Wang, H. 2006, *Solar Phys.* 237, 45.
 Falconer, D. A., Moore, R. L., and Gary, G. A. 2003, *Journal of Geophysical Research (Space Physics)* 108(A10), 11.
 Falconer, D. A., Moore, R. L., and Gary, G. A. 2006, *ApJ* 644, 1258.

- Harvey, K. L. and Zwaan, C. 1993, *Solar Phys.*148, 85.
Künzel, H. 1960, *Astronomische Nachrichten* 285, 271.
Lamb, D. A., DeForest, C. E., Hagenaar, H. J., Parnell, C. E., and Welsch, B. T. 2007, *ApJ*, submitted .
Linker, J. A., Lionello, R., Mikić, Z., and Amari, T. 2001, *JGR* 106, 25165.
Sammis, I., Tang, F., and Zirin, H. 2000, *ApJ*540, 583.
Schrijver, C. J. 2007, *ApJ*655, L117.
Welsch, B. T. 2006, *ApJ* 638, 1101.
Zirin, H. 1988, *Astrophysics of the Sun*, Cambridge Univ. Press, Cambridge.